Use of hyperelastic models and sliding connections to model the mechanical behavior of musculoskeletal structures

Gabriel B. Spínola[1], Humberto B. Coda[1], Rodrigo R. Paccola[1]

[1]*São Carlos School of Engineering, University of São Paulo*
Av. Trabalhador São Carlense, 400, 13560-590, São Carlos, SP, Brazil
gbspinola@usp.br, hbcoda@sc.usp.br, rbpaccola@sc.usp.br

Abstract. The demands of health care and well-being for humanity haven been requiring more detailed knowledge about movement and force generated by the musculoskeletal system. Structural analysis tools play an important role in that scenario, as *in vivo* and *in vitro* tests can be inconvenient. Thus, computational simulations are used to complement experimental these tests, offering cost and time advantages. This work aims to numerically model the behavior of the human upper limb, including muscle actions and joint movements, through a computational code based on the Positional Finite Element Method (PFEM). The proposed modelling treats muscle tissue as a composite material and uses Saint-Venant-Kirchhoff hyperelastic model for describing the stress-strain relationship. Sliding connections are employed to simulate the elbow joint's flexion and extension movements, and Lagrange multipliers are used for introducing kinematic conditions to the mechanical system. A numerical example of muscle contraction is employed to demonstrate the potential of the proposed model for analyzing biological structures.

Keywords: simulation, Positional Finite Element Method (PFEM), muscle, joints.

1 Introduction

The generation of movement and the production of force by the set of muscles, tendons, bones, and ligaments in various parts of the body have been a topic of high interest in research in recent years. In his review, Humphrey [1] points out that increasingly detailed and precise knowledge of the biomechanical behavior of these structures is required to meet the demands of health care and human well-being. Soft tissues exhibit complex behavior and are typically subjected to high levels of deformation. Added to this is the need to simultaneously describe the movement of joints triggered by muscle action taking into account contact and sliding patterns between bone surfaces and the variable position of the rotation axis [2].

The purpose of this work is to bring some contribution to the modelling of the human musculoskeletal system and the comprehension of its macro-mechanical behavior. The focus lies on the upper limb for representing the elbow movements of flexion and extension. A finite element model was developed including biomechanical properties of muscles, connective tissues, bones and joints.

The muscle behavior is divided into passive and active components, as done by many previous works, such as Böl *et al.* [3], Lamsfuss and Bargmann [4] and Baiocco et al. [5]. The first one responds elastically to external loads, while the second one has the ability to contract and produce force. Instead of assuming that each point in the muscle tissue is simultaneously occupied by both components [3], this work treats the muscle fibers and the connective tissues around them discretely, considering their behavior similarly to composite materials in engineering [4,5]. The various layers of connective tissue surrounding the muscle fibers form the matrix, while the fibers themselves constitute the composite's reinforcement. Besides providing reinforcement, the fibers also exhibit active behavior. The constitutive relationship in both matrix and fibers is described by Saint-Venant-

Kirchhoff hyperelastic model.

The elbow complex is chosen to be modeled along with the mechanical behavior of skeletal muscles and is treated as a hinge joint, meaning a planar joint that exhibits a single degree of freedom: rotation around an axis orthogonal to the plane of analysis [2]. Flexion and extension movements are rotations around the perpendicular axis to the plane of analysis, passing through the center of the joint. Studies reveal that this axis practically does not change position, which indicates a movement of pure rotation [6]. Besides, the motion that occurs in this joint is predominantly two-dimensional, with subtle deviation from the plane of analysis [7], which are neglected in this work.

Different types of finite elements are employed to discretize the biological structures. The triangular based prismatic element described by Carrazedo and Coda [8] are used for bones and soft tissues, while the activated truss element presented by Coda *et al*. [9] represents muscle fibers. To achieve the coupled behavior of a fiber-reinforced composite material, an immersion procedure of truss elements in a prismatic domain is addressed, following the work by Sampaio *et al*. [10]. The connection between bones in joints is obtained by the sliding connections formulation proposed by Siqueira *et al*. [11], allowing bones to display relative motion between each other while keeping contact.

To solve the mechanical problem, the Positional Finite Element Method (PFEM) [12,13] is adopted, a total Lagrangian directly non-linear geometric version of the traditional framework. In this approach, the unknowns are the element node's positions and the Newton-Raphson iterative procedure is used to solve the system of equilibrium equations.

2 Equilibrium equations and solution procedure

The equilibrium equations of a mechanical system are here obtained by the Principle of Stationary Mechanical Energy, which states that the system reaches equilibrium when the variation of the total mechanical energy is zero. Ogden [14] and Coda [15] are recommended for further details.

In static analysis, the total mechanical energy of a system with constraints, denoted by Π, can be written as follows:

$$\Pi = -\mathbb{P} + \mathbb{U} + \mathbb{C}. \tag{1}$$

$\mathbb{P}$ is the potential energy of external load, gathering the contributions of both concentrated and distributed conservative loads. $\mathbb{U}$ is the strain energy and corresponds to the integral of the specific strain energy u over the system's initial volume V_0. Employing Saint-Venant-Kirchhoff hyperelastic model, this portion of energy is written as:

$$\mathbb{U} = \int_{V_0} u \, dV_0 = \int_{V_0} \frac{1}{2} \boldsymbol{E}(\vec{Y}) : \mathfrak{C} : \boldsymbol{E}(\vec{Y}) \, dV_0, \tag{2}$$

in which $\mathfrak{C}$ is the fourth-order constitutive tensor of the adopted constitutive model and $\boldsymbol{E}$ is the Green-Lagrange strain tensor. Aiming at further use of the positional formulation for FEM, the strain tensor is taken as a function of the current nodal positions $\vec{Y}$, unknowns of the problem.

Finally, $\mathbb{C}$ is the constraint potential energy. This work imposes kinematic constraints to the system by Lagrange multipliers, so that this portion of energy can be written as:

$$\mathbb{C} = \vec{\lambda} \cdot \vec{c}(\vec{Y}), \tag{3}$$

in which $\vec{c}$ are constraint equations, also taken as a function of the nodal positions $\vec{Y}$, and $\vec{\lambda}$ are the Lagrange multipliers, unknowns of the problem as well.

The Principle of Stationary Mechanical Energy states that the system reaches equilibrium when the variation of mechanical energy is zero. Taking the variation of mechanical energy in relation to $\vec{Y}$ and $\vec{\lambda}$, and considering the variation of both variables is arbitrary, the equilibrium equations result:

$$-\begin{Bmatrix} \partial \mathbb{P}/\partial \vec{Y} \\ \vec{0} \end{Bmatrix} + \begin{Bmatrix} \partial \mathbb{U}/\partial \vec{Y} \\ \vec{0} \end{Bmatrix} + \begin{Bmatrix} \partial \mathbb{C}/\partial \vec{Y} \\ \partial \mathbb{C}/\partial \vec{\lambda} \end{Bmatrix} = -\vec{F}^{ext} + \vec{F}^{int}(\vec{Y}) + \vec{F}^{con}(\vec{Y}, \vec{\lambda}) = \vec{0}, \tag{4}$$

in which $\vec{F}^{ext}$, $\vec{F}^{int}$ and $\vec{F}^{con}$ are named vectors of external forces, internal forces and constraint forces, respectively.

The equilibrium equations are geometrically nonlinear and the Newton-Raphson method is employed to solve them. The solution procedure begins with the definition of the mechanical unbalanced vector $\vec{g}$ for a trial set of variables $\vec{Y}_0$ and $\vec{\lambda}_0$, according to the expression below:

$$\vec{g}(\vec{Y}_0, \vec{\lambda}_0) = -\vec{F}^{ext} + \vec{F}^{int}(\vec{Y}_0) + \vec{F}^{con}(\vec{Y}_0, \vec{\lambda}_0) = \vec{0}. \tag{5}$$

From the first-order Taylor series expansion of eq. (5) arises the system of equations for determining the correction values that updates the solution:

$$\begin{Bmatrix} \Delta\vec{Y} \\ \Delta\vec{\lambda} \end{Bmatrix} = -\boldsymbol{H}^{-1} \cdot \vec{g}(\vec{Y}_0, \vec{\lambda}_0), \tag{6}$$

in which $\boldsymbol{H}$ is the Hessian matrix for the trial variables. Considering that the external loads are conservative, this quantity can be written as:

$$\boldsymbol{H} = \left.\frac{\partial \vec{F}^{\boldsymbol{int}}}{\partial\{\vec{Y}, \vec{\lambda}\}}\right|_{\vec{Y}^0, \vec{\lambda}^0} + \left.\frac{\partial \vec{F}^{\boldsymbol{con}}}{\partial\{\vec{Y}, \vec{\lambda}\}}\right|_{\vec{Y}^0, \vec{\lambda}^0}. \tag{7}$$

The tentative solution is then updated by:

$$\begin{Bmatrix} \vec{Y} \\ \vec{\lambda} \end{Bmatrix} = \begin{Bmatrix} \vec{Y}_0 \\ \vec{\lambda}_0 \end{Bmatrix} + \begin{Bmatrix} \Delta\vec{Y} \\ \Delta\vec{\lambda} \end{Bmatrix}. \tag{8}$$

With the new trial vector, the new mechanical unbalanced vector $\vec{g}$ is calculated and the whole process is repeated until the error satisfies the following convergence criterion:

$$Error = \frac{\Delta\vec{Y}}{\vec{X}} \leq tolerance. \tag{9}$$

3 Positional approach for finite elements

In this section, the individual description of each element employed in this work is addressed first. Then, a strategy for embedding truss elements in a prismatic domain is presented. In addition to the works cited throughout the text ahead, Coda [15] is recommended for further details.

The triangular based prismatic element is a three-dimensional element generated from the extrusion of a triangular base, describe by Carrazedo and Coda [8]. In this work, the element's nodes are distributed according to a cubic approximation for the basis and a linear approximation for the extruded dimension. For such element, Green-Lagrange strain can be written as:

$$\boldsymbol{E_{prism}} = \frac{1}{2}(\boldsymbol{C} - \boldsymbol{I}) = \frac{1}{2}(\boldsymbol{A^T A} - \boldsymbol{I}). \tag{10}$$

In Equation (10), $\boldsymbol{C} = \boldsymbol{A^T A}$ is Cauchy strain tensor and $\boldsymbol{A}$ is the deformation gradient, which can be expressed as a function of nodal positions [8]. From that, the strain energy portion can be written as in eq. (2).

The activated truss element, in turn, has a linear approximation and its strain energy is only related to changes in length. It does not resist to transverse loads as well. The activation of this element corresponds to the ability to control the distance between its ends by imposing its length, as presented by Coda *et al.* [9]. For the uniaxial description adopted, Green-Lagrange strain assumes the following format:

$$E_{truss} = \frac{1}{2}\left(\frac{L^2}{{L_{0n}}^2} - 1\right), \tag{11}$$

in which L_{0n} is the initial natural length of the element, corresponding to the initial length plus an increment ΔL, that is:

$$L_{0n} = L_0 + \Delta\mathrm{L}. \tag{12}$$

The parameters L_0 and L are, respectively, the initial length and the current length and are both written as a function of nodal positions [9]. Thus, Green-Lagrange strain for the truss element, eq. (11), is expressed in terms of positions and can be applied in eq. (2).

The numerical strategy to embed truss elements into prismatic elements is an extension to the three-dimensional domain of the procedure proposed by Sampaio *et al.* [10]. This technique consists of writing the truss nodes' positions as a function of the prismatic element nodes' positions in both initial and current configurations:

$$\overline{\mathrm{X}}_j^k = \psi_l(\vec{\xi}^k)\hat{X}_j^l, \tag{13}$$

$$\overline{\mathrm{Y}}_j^k = \psi_l(\vec{\xi}^k)\hat{Y}_j^l. \tag{14}$$

$\psi_l(\vec{\xi}^k)$ are the prismatic element's shape functions evaluated on the dimensionless coordinates $\vec{\xi}$ of the truss node k. The symbol $(\bar{\bullet})$ represents the parameters related to the truss element, while $(\hat{\bullet})$ represents the parameters related to the prismatic elements.

The strain energy stored in a reinforced body is equal to the sum of the strain energy stored in the matrix and the bars. Thus, once truss nodes' positions are written as eq. (13) and eq. (14), the vector of internal forces and the Hessian matrix are given by:

$$\left(F_i^l\right)^{int} = \frac{\partial \mathbb{U}}{\partial \hat{Y}_i^l} = \frac{\partial\left(\hat{\mathbb{U}} + \overline{\mathbb{U}}\right)}{\partial \hat{Y}_i^l} = \frac{\partial \hat{\mathbb{U}}}{\partial \hat{Y}_i^l} + \frac{\partial \overline{\mathbb{U}}}{\partial \overline{Y}_j^k}\frac{\partial \overline{Y}_j^k}{\partial \hat{Y}_i^l} = \left(\hat{F}_i^l\right)^{int} + \left(\bar{F}_i^k\right)^{int}\psi_l(\vec{\xi}^k), \tag{15}$$

$$H_{ilgz} = \frac{\partial\left(\hat{\mathbb{U}} + \overline{\mathbb{U}}\right)}{\partial \hat{Y}_i^l \partial \hat{Y}_g^z} = \frac{\partial \hat{\mathbb{U}}}{\partial \hat{Y}_i^l \partial \hat{Y}_g^z} + \frac{\partial \overline{\mathbb{U}}}{\partial \overline{Y}_j^k \partial \overline{Y}_m^n}\frac{\partial \overline{Y}_j^k}{\partial \hat{Y}_i^l}\frac{\partial \overline{Y}_m^n}{\partial \hat{Y}_g^z} = \hat{H}_{ilgz} + \bar{H}_{ikgn}\psi_l(\vec{\xi}^k)\psi_z(\vec{\xi}^n). \tag{16}$$

It is important to note that this strategy allows the insertion of truss elements in any position of the domain without increasing the problem's number of degrees of freedom. Besides, it ensures perfect adherence between the truss elements and the matrix [10].

4 Sliding connections

Sliding connections are the joints between two surfaces that allow them to slide over one another without losing contact neither overlapping each other. This kind of attachment can be taken into account in the analysis of structural systems by introducing the constraint potential energy portion to the mechanical energy, as it is done in section 2.

Considering a planar system discretized in finite elements, a sliding connection corresponds to a sliding node $\hat{P}$ that is constrained to move over a path, associated to a unidimensional finite element called 'path element'. The contact point over the path element is referred to as $\bar{P}$ and its position is defined by an arc-length parameter s_P, which is taken as an independent variable of the problem [11].

To ensure that the sliding node keeps contact to the path, the coordinates of point $\hat{P}$ must be equal to the coordinates of point $\bar{P}$. As finite elements discretize the geometry of the bodies, this condition can be directly expressed by using their nodal positions. Thus, the constraint equations $\vec{c}$ can be written as follows:

$$c_i = \hat{Y}_i^P - \phi_l(\xi_P)\bar{Y}_i^l = 0_i. \tag{17}$$

Equation (17) is valid for any pair of points in contact. The index $i = 1{,}2$ represents the plane's orthogonal directions, $\hat{Y}_i^P$ is the current position of point $\hat{P}$, $\bar{Y}_i^l$ is the current position of the l nodes from the path element, $\phi_l(\xi_P)$ are the shape functions associated with the nodes of the path element and ξ_P is the dimensionless coordinate of the contact point. The approximation $\bar{Y}_i^P = \phi_l(\xi_P)\bar{Y}_i^l$ was used for the contact point's position on the path element.

This work models the sliding among triangular based prismatic elements through a coupling strategy between path elements and prismatic elements in the contact regions, based on Siqueira *et al.* [11]. By using nodal positions as parameters for both elements, the coupling occurs by kinematical compatibility of these variables, associating their degrees of freedom. Sliding nodes and path elements are defined over the edge of prismatic elements that slide against each other, ensuring that all nodes of a sliding edge are restricted to move over the set of path elements.

The coupling strategy represents the sliding in the plane defined by x_1 and x_2 axes. Path elements are defined on both entrance and exit planes of x_3 axis, as depicted in Fig. 1. The adopted path element has a cubic approximation, to minimally accommodate the shape of the prismatic element on which they are defined.

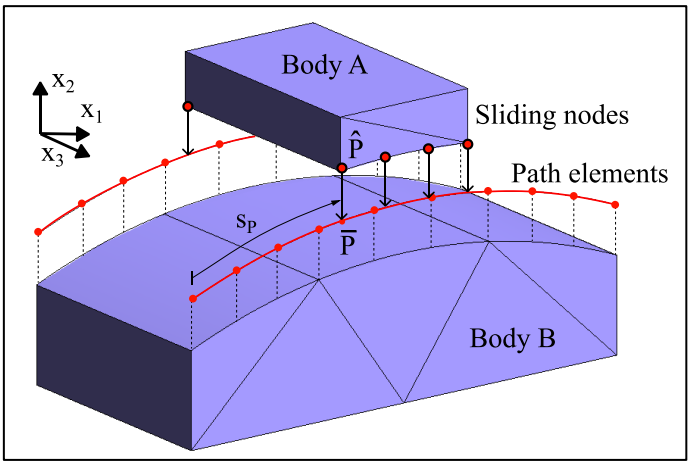

Figure 1. Coupling between prismatic elements and path elements (contact points apart for clarity).

5 Numerical example: the upper limb simulation

Saint-Venant-Kirchhoff hyperelastic constitutive model and the sliding connections formulation is applied on the modelling of biological structures. The system chosen in this work is the upper limb of the human body and the adopted geometry is inspired on the images of the right upper limb of a 26-year-old female patient, obtained from a computed tomography (CT) scan [16]. The model is presented on Fig. 2.

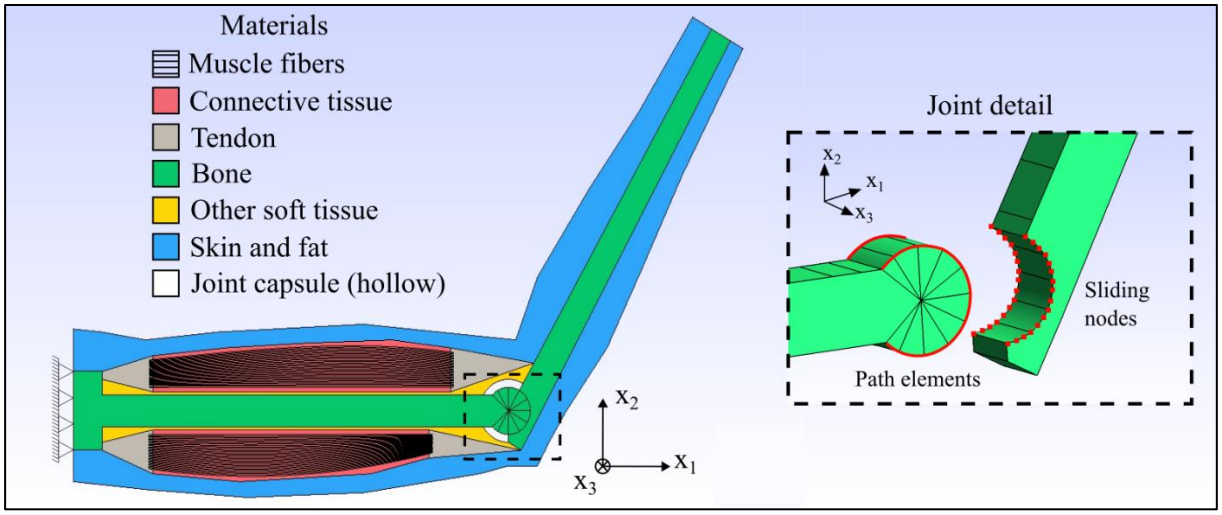

Figure 2. Human upper limb model and joint detail (contact points apart for clarity).

The domain is discretized by triangular based prismatic elements and the fibers are composed of truss elements, inserted in mid-plan of the prismatic matrix. The mechanical behavior of all materials is described by Saint-Venant-Kirchhoff model. The elastic moduli are 0.2415 MPa for connective tissue (red) [10], 1000 MPa for tendon (gray) [17], 17500 MPa for bone (green) [17], 4.65 MPa for fibers [10] and 0.1 MPa for other soft tissue (yellow), skin and fat (blue). Poisson's ratio is made zero for all materials.

The relative motion between bone materials in the elbow joint is represented by the sliding connections formulation. Path elements are introduced on the right edges of humerus, while sliding nodes are inserted at all nodes contained within the sliding boundary of the forearm bone end in contact with the humerus.

In the first analysis, a length variation of -0.25 mm is applied to all fiber in the anterior compartment, which is equivalent of approximately a 12.5% reduction of the initial fiber length. Meanwhile, the fibers in the posterior compartment are free to stretch. In the second analysis, a length variation of -0.4 mm is applied to all fibers in the

posterior compartment (approximately 20% of initial length), while the fibers in the anterior compartment are free to stretch.

As expected, fiber activation in the anterior compartment causes elbow flexion. On the other hand, fiber activation in the posterior compartment generates elbow extension. Upon removing the imposed length variations, the structure returns to the initial configuration. Displacements in the x_1 direction are depicted in Fig. 3, which also details small areas of the model where the material reverses its orientation. Although this phenomenon is physically inadequate, Saint-Venant-Kirchhoff hyperelastic model allows it to occur when the regime of moderate strains is exceeded [14,15].

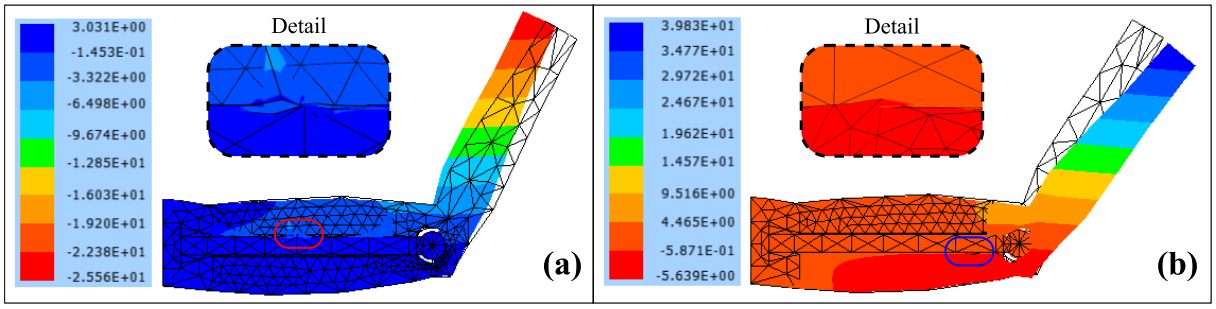

Figure 3. Displacements in the x_1 direction for contraction in the (a) anterior compartment and (b) posterior compartment, detailing areas where orientation reversion occurs.

Cauchy normal stress in the x_1 direction is illustrated in Fig. 4 for both analyses. All fibers are submitted to traction, which means that muscle contraction tensions not only the contracted fibers of one compartment, but also the fibers in the opposite compartment, which undergo passive stretching. The stresses occur with greater intensity in the contracted fibers, responsible for performing the limb movement. Regarding the matrix muscle materials, compression stresses are developed in the connective tissue of the compartment where contraction occurs, while tensile stresses are observed in the tendons. In the opposite compartment, both the muscular connective tissue and the tendons are subjected to tensile stresses.

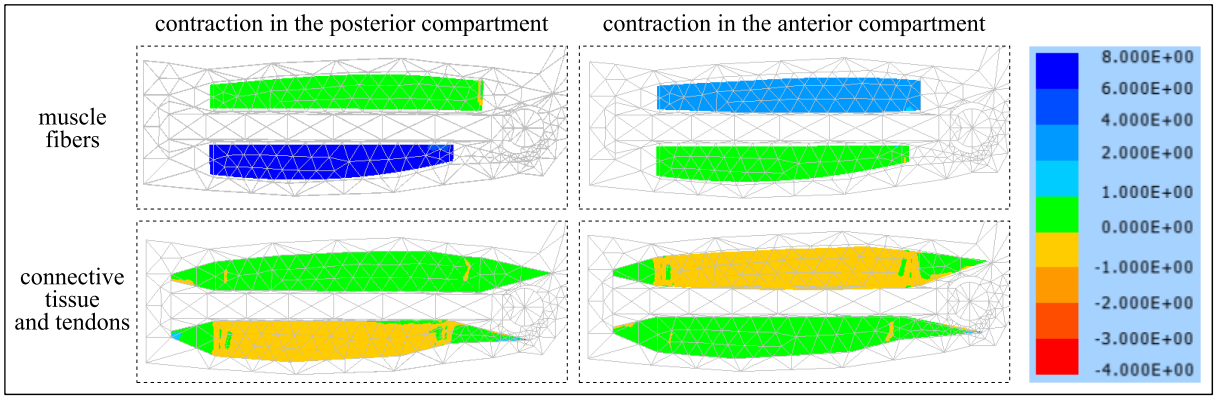

Figure 4. Cauchy normal stress in the x_1 direction

The distal arm bone surface maintains contact with the proximal forearm bone surface during the whole process of both analyses, sliding over one another for flexion and extension movements. The contact forces in the sliding nodes are directed towards the axis of rotation of the forearm, positioned at the center of the elbow. This is consistent with the proposed geometric modeling, which displays the paths elements and the sliding nodes as two concentric circle arcs.

6 Conclusions

The simulation of the upper limb reveals that it is possible to describe the planar mechanical response of human body limbs by the content here discussed. The sliding connections formulation proved to be efficient in constraining two bodies to move along one another without losing contact and, therefore, representing a human joint. Saint-Venant-Kirchhoff hyperelastic constitutive model works well within moderate strains, but becomes inconsistent when describing the mechanical behavior in large strains, therefore not suiting many problems involving soft tissues. The computational code's potential for analyzing biological structures as a composite material (matrix/fiber) in three-dimensional space and for applying more complex constitutive models is also confirmed.

Acknowledgements. The authors acknowledge the support provided by Conselho Nacional de Desenvolvimento Científico e Tecnológico (CNPq) and Coordenação de Aperfeiçoamento de Pessoal de Nível Superior – Brasil (CAPES) – Finance Code 001.

Authorship statement. The authors hereby confirm that they are the sole liable persons responsible for the authorship of this work, and that all material that has been herein included as part of the present paper is either the property (and authorship) of the authors, or has the permission of the owners to be included here.

References

[1] J. D. Humphrey. "Review Paper: Continuum biomechanics of soft biological tissues". Proceedings of the Royal Society of London. Series A: Mathematical, Physical and Engineering Sciences, v. 459, n. 2029, p. 3–46, 2003.
[2] C. A. Oatis. Kinesiology: the mechanics and pathomechanics of human movement. 2. ed. Lippincott Williams & Wilkins, 2009.
[3] M. Böl, M. Sturmat and C. Weichert. "A new approach for the validation of skeletal muscle modelling using MRI data". Comput Mech, vol. 47, pp. 591–601, 2011.
[4] J. Lmasfuss and S. Bargmann. "Skeletal muscle: Modeling the mechanical behavior by taking the hierarchical microstructure into account". *Journal of the Mechanical Behavior of Biomedical Materials*, v. 122, pp. 104670, 2021.
[5] M. H. Baiocco, H. B. Coda and R. R. Paccola. "A simple way to model skeletal muscles by FEM". In: Associação Brasileira de Ciências Mecânicas, 22nd International Congress of Mechanical Engineering (COBEM 2013), pp. 9227–9233.
[6] E. Y. Chao and B. F. MORREY. "Three-dimensional rotation of the elbow". *Journal of Biomechanics*, v. 11, n. 1–2, pp. 57–73, 1978.
[7] G. H. Callaway *et al*. "Biomechanical evaluation of the medial collateral ligament of the elbow". *The Journal of bone and joint surgery*. American volume, v. 79, n. 8, pp. 1223–1231, 1997.
[8] R. Carrazedo and H. B. Coda. "Triangular based prismatic finite element for the analysis of orthotropic laminated beams, plates and shells". *Composite Structures*, v. 168, pp. 234–246, 2017.
[9] H. B. Coda, A. P. Silva and R. R. Paccola. "Alternative active nonlinear total Lagrangian truss finite element applied to the analysis of cable nets and long span suspension bridges". *Latin American Journal of Solids and Structures*, v. 17, n. 3, pp. 268, 2020.
[10] M. S. M. Sampaio, R. R. Paccola and H. B. Coda. "Fully adherent fiber–matrix FEM formulation for geometrically nonlinear 2D solid analysis". *Finite Elements in Analysis and Design*, v. 66, pp. 12–25, 2013.
[11] T. M. Siqueira, E. A. Rodríguez and H. B. Coda. "Dynamical analysis of sliding connections with mesh independent roughness by a total Lagrangian FEM". *Latin American Journal of Solids and Structures*, v. 19, n. 7, pp. 1–31, 2022.
[12] J. Bonet *et al*. "Finite element analysis of air supported membrane structures". *Computer Methods in Applied Mechanics and Engineering*, v. 190, n. 5–7, pp. 579–595, 2000.
[13] H. B. Coda. Análise não linear de geométrica de sólidos e estruturas: uma formulação posicional baseada no MEF. PhD Thesis, University of São Paulo, 2003.
[14] R. W. Ogden. *Non-linear Elastic Deformations*. Dover Publications, 1997.
[15] H. B. Coda. *O Método dos Elementos Finitos Posicional: sólidos e estruturas - não linearidade geométrica e dinâmica*. EDUSP, 2018.
[16] J. J. Cabibihan, M. K. Abubasha and N. Thakor. "A Method for 3-D Printing Patient-Specific Prosthetic Arms with High Accuracy Shape and Size". *IEEE Access*, v. 6, pp. 25029–25039, 2018.
[17] Y. C. Fung. *Biomechanics: mechanical properties of living tissues*. 2. ed. Springer, 1993.